CALCULATION OF THE VISCOUS RESISTANCE OF BODIES OF REVOLUTION

by

A. Nakayama and V. C. Patel

Sponsored by
General Hydromechanics Research Program
of the Naval Ship Systems Command
Naval Ship Research and Development Center
Contract No. N00014-68-A-0196-0002

IIHR Report No. 151

Iowa Institute of Hydraulic Research
The University of Iowa
Iowa City, Iowa

October 1973

CALCULATION OF THE VISCOUS RESISTANCE OF BODIES OF REVOLUTION

by

A. Nakayama and V. C. Patel

Sponsored by
General Hydromechanics Research Program
of the Naval Ship Systems Command
Naval Ship Research and Development Center
Contract No. N00014-68-A-0196-0002

IIHR Report No. 151

Iowa Institute of Hydraulic Research
The University of Iowa
Iowa City, Iowa

October 1973

ABSTRACT

The flow in the tail region of a body of revolution is a complex one since there the boundary layer often grows to a thickness many times the local radius of the body and there results a strong interaction between the boundary layer and the external potential flow. The influence of making simplifying assumptions concerning the flow in this region in conventional drag-calculation methods is discussed, and assessed by incorporating a method which takes into account the effects of the thick axisymmetric boundary-layer near the tail in an approximate manner. It is shown that this modification leads to a drag-calculation method which gives consistently accurate prediction of the viscous resistance of a wide variety of bodies of revolution.

ACKNOWLEDGEMENT

This paper is based upon research conducted under the General Hydromechanics Research Program of the Naval Ship Systems Command, technically administered by the Naval Ship Research and Development Center, under Contract N00014-68-A-0196-0002.

LIST OF CONTENTS

LIST OF TABLES

LIST OF FIGURES

LIST OF SYMBOLS

C_D drag coefficient ($= \frac{D}{\frac{1}{2}\rho U_\infty^2 V^{2/3}}$ unless otherwise is stated)

C_p pressure coefficient ($= \frac{p - p_\infty}{\frac{1}{2}\rho U_\infty^2}$)

C_P prismatic coefficient ($= \frac{4V}{\pi d^2 L}$)

d maximum diameter of a body

D viscous drag

H shape factor ($= \frac{\delta_1}{\delta_2}$)

L total length of a body

m position of r_{max} ($= \frac{X_m}{L}$)

p pressure

p_∞ undistrubed freestream pressure

r distance to the axis of a body of revolution

r_o local radius of a body of revolution

r_{max} maximum local radius of a body of revolution

r_n nose radius

r_t tail radius

R_e Reynolds number ($= \frac{U_\infty L}{\nu}$)

R_n nondimensional nose radius ($= \frac{r_n L}{d^2}$)

R_t nondimensional tail radius ($= \frac{r_t L}{d^2}$)

R_x Reynolds number based on x ($= \frac{U_e X}{\nu}$)

R_δ Reynolds number based on δ ($= \frac{U_e \delta}{\nu}$)

R_θ Reynolds number based on δ_2 ($= \frac{U_e \delta_2}{\nu}$)

S total surface area of a body

u'	root-mean-square value of the velocity fluctuations in the freestream
U	velocity component in x-direction
U_e	velocity component in x-direction at the edge of the boundary layer
U_∞	undisturbed freestream velocity
V	volume of a body
x	distance along the surface of a body from the nose
X	axial distance from the nose
X_m	axial distance to the point of maximum radius
X_{tr}	axial distance to the transition from laminar to turbulent boundary layer
y	distance to a point normal to the surface
δ	boundary layer thickness
δ_1	displacement thickness
δ_2	momentum thickness
Δ_1	displacement area
Δ_2	momentum area
λ	pressure gradient parameter ($= \frac{\delta_2^2}{\nu} \frac{dU_e}{dx}$)
Λ	pressure gradient parameter ($= \frac{\delta^2}{\nu} \frac{dU_e}{dx}$)
ν	kinematic viscosity of a fluid
ρ	density of a fluid

CALCULATION OF THE VISCOUS RESISTANCE OF BODIES OF REVOLUTION

I. INTRODUCTION

There has always been a certain amount of ambiguity in the calculation of the viscous resistance of a body of revolution stemming from the treatment of the flow in the region near the tail of the body. In order to calculate the resistance in the absence of separation, either by the application of the well know Squire-Young method or by the continuation of a boundary-layer type calculation through the near wake to predict the momentum deficit in the far wake, it is necessary to know the characteristics of the boundary layer at the tail and also the velocity just outside the boundary layer at this point. As pointed out recently by Patel, Nakayama and Damian (1973), the flow in the tail region of the body (the rear 10 to 15 percent of the body length, say) requires special attention for two reasons: (a) the usual thin boundary-layer approximations cease to apply in this region since the boundary layer often grows to a thickness many times the local radius of the body, and (b) there exists substantial interaction between the thick boundary layer and the potential flow outside it, so that potential-flow theory, by itself, predicts neither the pressure distribution on the surface nor the freestream velocity distribution which the boundary layer sees. If the pressure distribution obtained from potential-flow theory is used to calculate the boundary layer development right up to the tail two difficulties arise: (a) premature separation may be encountered owing to the fact that the potential-flow pressure gradients are much larger than those actually observed experimentally, and (b) the existence of a stagnation point at the tail, and consequently zero freestream velocity, leads to a failure of the Squire-Young method for predicting the momentum deficit in the far wake. In previous methods for the calculation of drag, such as those of Granville (1953), Cebeci, Mosinskis and Smith (1970) and Parsons and Goodson (1972), these difficulties have been avoided by continuing the boundary-layer calculation into the tail region using some pressure distribution obtained by arbitrarily extrapolating the potential-flow pressure distribution from further upstream. However, only the usual thin boundary-layer calculation methods have been

used thus far to determine the required parameters of the boundary layer at the tail. The influence of these assumptions on the final prediction of the resistance of bodies of revolution remains undetermined. The complex nature of the flow in the tail region has been discussed recently by Patel (1973a) and it appears that a satisfactory solution of the problem must await further investigations of the influence of strong transverse curvature on turbulent boundary layers and also the development of procedures for the calculation of the interaction between the boundary layer and the potential flow. As a first step towards assessing the importance of the flow in the tail region, however, an integral method proposed recently by Patel (1973b) for the calculation of THICK, axisymmetric, turbulent boundary layers has been incorporated in the more or less conventional drag calculation scheme. This paper describes the results of that study.

A computer program has been developed for the calculation of the viscous resistance of a streamlined body of revolution placed axially in a uniform incompressible stream. When the dimensions of the body and the Reynolds number are specified, the program first finds the potential-flow pressure distribution on the body surface. The laminar boundary layer over the nose portion of the body is then calculated. This is terminated at the point where transition to turbulent flow takes place. The location of the transition point may be prescribed *a priori*, or it may be determined by the use of any one of the transition criteria available in the literature. Some of the well known criteria have been employed in this work in order to evaluate their relative merits and also to study the influence of the position of transition on the resistance of the body. Beyond transition, the development of the turbulent boundary layer is calculated using the method of Patel mentioned earlier. Finally, the resistance of the body is calculated using the Squire-Young method in conjunction with the shape parameter and the momentum thickness predicted in the tail region. Herein lies another departure from procedures used previously. Instead of using some extrapolated pressure distribution in the tail region, the boundary layer calculations are performed using the potential-flow pressure distribution. The difficulties associated with this procedure were, however, avoided by employing a Squire-Young type formula after each step in the boundary layer calculation over the last ten percent of the body length. The successive values of "drag coefficient" obtained in this manner were found to increase up to some point

and decrease thereafter as the boundary layer calculation approached the tail of the body. The required drag coefficient of the body was simply taken to be the maximum value. Comparisons made with the values obtained by using the experimentally measured pressure distribution in place of the potential-flow pressure distribution suggested that this procedure yields acceptable results. The new procedure is therefore more satisfactory than previous ones in that it avoids the need to guess the actual pressure gradients experienced by the boundary layer in the tail region.

The resistance coefficients calculated by the present method have been compared with available experimental data for a wide variety of bodies of revolution. These comparisons show that the resistance of bodies of revolution can now be predicted with considerable accuracy provided the exact location of the transition point is known or can be found.

II. DETAILS OF THE METHOD OF CALCULATION

The various elements which constitute the present drag calculation scheme were outlined in the Introduction. With the exception of the turbulent boundary-layer calculation method and the application of a Squire-Young type formula, the calculation procedures used here are quite well known. We shall therefore describe these briefly in the following sections, elaborating only upon those aspects which are new.

A. The Potential Flow Calculation: There are of course a number of methods available for the solution of the potential flow on an axisymmetric body placed in a uniform axial stream. Amongst these, the method developed by Landweber (1959), in which the problem is reduced to the solution of a Fredholm integral equation of the first kind, appeared to be the best suited for the present study since it is relatively simple to use. The general derivation of the integral equation and a suitable iterative numerical procedure for its solution have been described in detail by Landweber. This procedure was utilized, with some minor modification, in the present study. Although Gauss quadrature of order 16 (i.e. the use of 16 coordinate points to specify the shape of the body) originally recommended gave acceptable results, the order was changed to 24 so that a simple interpolation formula could be used with sufficient accuracy to find the required pressure gradients in the boundary-layer calculations. A convergence criterion was also incorporated

in order to stop the iteration procedure when a desired level of accuracy was reached. During the course of this work it was observed that to obtain reliable and smooth pressure distributions the coordinates of the body had to be specified with considerable precision.

The pressure distributions calculated using this method are compared with four sets of experimental data in Figures 1(a) through 1(d). The body shapes are also shown in these figures. The pressure coefficient, C_p, is defined as follows:

$$C_p = \frac{p - p_\infty}{\frac{1}{2}\rho U_\infty^2} \quad , \tag{1}$$

where p is pressure at any point on the body, U is velocity, ρ is density and the subscript ∞ refers to values in the undisturbed stream. It will be seen that the agreement between experiment and potential-flow theory is satisfactory over most of the body surface in the first three cases shown. In the last case, namely that of Cornish and Boatwright (1960), the lack of close agreement may be due to the fact that these measurements were made on a full-scale airship which was not truly axisymmetric owing to the presence of control surfaces. The departure of the experimental pressure distribution from potential-flow theory in the tail region, commented upon earlier and attributed to the strong interaction between the boundary layer and the external flow, is well illustrated by the experiments of Lyon (1934) shown in Figures 1(b) and 1(c).

B. Laminar Boundary Layer Development: For the calculation of the laminar boundary layer over the nose portion of the body, the method of Thwaites (1949), as modified by Rott and Crabtree (1952) for axisymmetric flow, was employed. In this method, the momentum-integral equation is reduced to a simple quadrature formula of the form

$$\delta_2^2 = 0.47\nu r_o^{-2} U_e^{-6} \int_0^x r_o^2 U_e^5 dx \quad , \tag{2}$$

where δ_2 is the momentum thickness of the boundary layer defined in the manner appropriate for axisymmetric flow (see equation (6) later), ν is kinematic viscosity, x is the distance measured along the body surface from the nose, $r_o(x)$ is the radius distribution of the body and $U_e(x)$ is the freestream

velocity outside the boundary layer obtained from the potential-flow pressure distribution calculated previously, viz.

$$\frac{U_e}{U_\infty} = (1 - C_p)^{\frac{1}{2}} \quad . \tag{3}$$

Note that the small but finite value of the momentum thickness at the nose of the body ($x = 0$) is ignored.

The momentum thickness calculated from equation (2) was used in the prediction of transition to turbulent flow in the manner described in the next section. For transition criteria which require information concerning laminar boundary-layer parameters other than the momentum thickness, however, such parameters were found from the singly-infinite family of velocity profiles of Pohlhausen and the calculated momentum thickness.

C. Prediction of Transition: Numerous empirical or semi-empirical criteria have been proposed in the past for the prediction of transition from laminar to turbulent flow. From these, the criteria due to Michel (1951), Granville (1953), Crabtree (1958), van Ingen (1956), van Driest and Blumer (1963), Jaffe, Okamura and Smith (1970), and Hall and Gibbings (1972) were examined during the course of this work but, for reasons of simplicity, only the four listed below were finally incorporated in the drag calculation scheme. The parameters which are required for the calculation of the transition point according to these criteria are also listed.

TRANSITION CRITERION	PARAMETERS
Michel (1951)	R_θ, R_x
Granville (1953)	R_θ, Λ, ΔR_θ, $\bar{\Lambda}$, u'/U_∞
Crabtree (1958)	R_θ, λ
van Driest & Blumer (1963)	R_δ, Λ, u'/U_e

Here, u' is the root-mean-square value of the velocity fluctuations in the freestream; R_θ, R_δ, and R_x are local Reynolds numbers defined by

$$R_\theta = \frac{U_e \delta_2}{\nu} \quad , \quad R_\delta = \frac{U_e \delta}{\nu} \quad , \quad R_x = \frac{U_e x}{\nu} \quad ; \tag{4}$$

and, Λ and λ are pressure-gradient parameters defined by

$$\Lambda = \frac{\delta^2}{\nu}\frac{dU_e}{dx}\ , \quad \lambda = \frac{\delta_2^{\,2}}{\nu}\frac{dU_e}{dx}\ , \tag{5}$$

where δ is the physical thickness of the boundary layer. The parameters ΔR_θ and $\bar{\Lambda}$ appearing in the method of Granville are, respectively, the change in R_θ and the average value of Λ between the point of neutral stability as indicated by stability theory and the point of self-excited transition.

In the method of van Driest and Blumer the value of R_δ at transition is related to Λ and u'/U_e via a simple equation. In the other three cases the value of R_θ at transition is obtained from the other parameters by the use of correlation curves presented graphically by the originators. These curves were read into the computer in the form of tables and were used in conjunction with suitable interpolation formulae.

The four criteria listed above were used, in turn, to determine the transition point. At this point the calculation of the laminar boundary layer was terminated and the turbulent boundary-layer calculations described in the following section were initiated. Calculations were also performed using the experimentally observed transition point when this was known.

D. Turbulent Boundary Layer Calculation: In order to calculate the development of the turbulent boundary layer, values have to be assigned to the parameters R_θ and H immediately following transition. The value of R_θ presents no problem in the case of natural transition since it remains constant across transition. The value of H corresponding to this R_θ and the local pressure gradient was then inferred from the relations between the various parameters given by Nash (1965) for equilibrium boundary layers and the skin-friction formula of Thompson (1965). It should be pointed out here that in cases where transition is promoted by artificial finite disturbances, such as boundary-layer trips, boundary-layer calculations should be performed after taking into account the additional momentum thickness due to the transition devices or using the experimental values of H and R_θ downstream of transition. This procedure was not, however, necessary in the cases treated here.

The turbulent boundary-layer calculation method used here is described in detail by Patel (1973b). This method is capable of predicting the development of thin as well as thick axisymmetric boundary layers, and for thin boundary layers it reduces identically to the extension of the method of Head (1958) proposed for axisymmetric flow by Shanebrook and

Sumner (1970). The thick boundary layer effects over the tail of the body are taken into account in an approximate manner by the use of (a) the freestream velocity distribution implied by the pressure distribution on the surface rather than the actual freestream velocity distribution that exists as a result of the interaction between the boundary layer and the potential flow, and (b) generalized forms of Head's entrainment and shape-parameter relations. Some calculations were also performed using the Shanebrook and Sumner form of Head's method into the tail region in order to ascertain the influence of taking the thick boundary-layer effects into account.

E. Prediction of Drag Coefficient: The turbulent boundary-layer calculation method described above predicts, amongst other things, the growth of the displacement and momentum thicknesses defined in a manner appropriate to axisymmetric boundary layers, viz.

$$\delta_1 = \int_0^{\delta} (1 - \frac{U}{U_e}) \frac{r}{r_o} dy \ , \quad \delta_2 = \int_0^{\delta} \frac{U}{U_e}(1 - \frac{U}{U_e}) \frac{r}{r_o} dy \ , \tag{6}$$

where y is the distance measured normal to the surface, r is the distance from the axis of the body and U(y) is the velocity distribution in the boundary layer. Since r_o becomes zero at the tail of the body, δ_1 and δ_2 become infinite there. However, the values of the displacement and momentum areas, defined as

$$\Delta_1 = 2\pi r_o \delta_1 \ , \quad \Delta_2 = 2\pi r_o \delta_2 \tag{7}$$

can be found, and these remain finite at the tail. For a body of revolution the Squire-Young drag formula, as given by Young (1939), may be written

$$C_D = \frac{2\Delta_2}{S} \left(\frac{U_e}{U_\infty}\right)^{\frac{1}{2}\left(\frac{\Delta_1}{\Delta_2} + 5\right)} \ , \tag{8}$$

where

$$C_D \equiv \frac{D}{\frac{1}{2}\rho U_\infty^2 S} \tag{9}$$

is the drag coefficient, D is the drag force on the body and S is a characteristic area of the body (e.g. the maximum cross-sectional area or the total surface area). All quantities in equation (8) are to be evaluated at the tail of the body. A formula somewhat similar to equation (8) has also been suggested by Granville (1953):

$$C_D = \frac{2\Delta_2}{S} \left(\frac{U_e}{U_\infty}\right)^{\frac{1}{8}\left[7\left(\frac{\Delta_1}{\Delta_2} + 2\right) + 3\right]} . \qquad (10)$$

This latter formula was used in the drag calculations described below.

As mentioned earlier, the use of the potential-flow pressure distribution in the calculation of the boundary layer development means that neither equation (8) nor equation (10) can be used to predict the drag coefficient since, according to the potential flow, $U_e = 0$ at the tail. To circumvent this difficulty, equation (10) was used after every step in the turbulent boundary-layer calculation beyond axial distances greater than 90 percent of the length of the body. Thus C_D was calculated after every step in the boundary layer calculation as if the body were terminated there. Figure 2 shows the results of such calculations for the two models tested experimentally by Lyon (1934). Also shown in this figure are the values of C_D predicted in this manner using the experimental pressure distributions which, as shown in Figures 1(b) and 1(c), are significantly different from the potential-flow solutions over the tail region of the bodies It will be seen that the use of the experimental pressure distribution leads to an unambiguous value for the drag coefficient as the tail is approached in both cases. At the present time, however, a theoretical method does not exist for the prediction of the real pressure distribution in the tail region. Drag prediction procedures must therefore rely only upon the potential-flow theory. Figure 2 shows that the successive values of C_D obtained by using the potential-flow pressure distribution reach a maximum somewhat ahead of the tail and then decrease as the tail is approached. The break in the C_D curve for Model B of Lyon indicates that the boundary layer calculation predicted separation at $X/L = 0.988$ although no separation was observed at this point in the experiments. The solution to the problem adopted here was simply to accept the maximum value as the final drag coefficient of the body. This assumption was considered reasonable since the remaining part of the body contributes little to the frictional resistance while its

contribution to the pressure drag is taken into account, in a rather indirect way, by the use of the Squire-Young method since the flow over the reamining part is then regarded as a part of the wake.

The simple approach described above led to acceptable results for the drag coefficient even when the boundary layer calculations indicated separation some distance ahead of the tail. This approach broke down in a number of cases, however, when the thick boundary-layer method was replaced by the thin boundary-layer method of Shanebrook and Sumner (1970). Figure 3 illustrates the influence of using these two methods on the successive values of the drag coefficient for the Akron model of Freeman and Model B of Lyon. From this we see that in Freeman's case the thin boundary-layer method gives an abnormally rapid increase of C_D as the tail is approached, and does not display the maximum found in the other cases, whereas the thick boundary-layer method leads to a well-defined maximum value which agrees with the experimental value. A rapid monotonic increase in the successive values of C_D was also observed for a number of bodies of revolution in the recent study of Parsons and Goodson (1972) who employed a thin boundary-layer calculation method together with extrapolated pressure distributions for the tail region. It appears therefore that the use of the conventional thin boundary-layer methods for the flow in the tail region may lead, under certain circumstances depending upon the shape of the body, to a gross over-estimation of the drag coefficient.

III. RESULTS AND DISCUSSION

Before describing the results of the overall drag calculations it is useful to examine, very briefly, the performance of the various components of the complete drag-calculation procedure. From the comparisons shown in Figure 1 and discussed in Section IIA it was concluded that the method of Landweber gives satisfactory prediction of the potential-flow pressure distribution. To assess the accuracy of the boundary layer calculations and the various transition criteria employed here, comparisons have been made with the experimental data from the four bodies of revolution considered earlier, namely the Airship Akron model of Freeman (1932a, b), Models A and B of Lyon (1934), and the U.S. Navy ZS2G-1 Airship tested by Cornish and Boatwright (1960).

From the transition results summarized in Table 1 it will be seen that no single criterion predicts the experimental transition point with desired accuracy. The criteria of Granville, and van Driest and Blumer, predict transition correctly in two out of the three cases where transition was observed experimentally, while the methods of Michel and Crabtree give agreement with only one case. In view of this, the boundary layer calculations performed using only the experimentally observed transition point and one other transition criterion are shown in Figures 4 through 7. Also shown in these figures are the results of the calculations in which the thick turbulent boundary-layer method of Patel (1973b) was replaced by the thin turbulent boundary-layer method of Shanebrook and Sumner (1970). The calculations shown in Figures 4 through 6 employed the potential-flow pressure distribution, but due to the disagreement between the experimental and the potential-flow pressure distributions on the U.S. Navy Airship, attributed earlier to a lack of axial symmetry, the calculations in Figure 7 were performed using the pressure distribution measured at the larger of the two Reynolds numbers.

The comparisons between the calculations and the experimental data suggest that the development of the laminar and the turbulent boundary layers is predicted satisfactorily, at least in the range covered by the measurements, provided the point of transition is either know or predicted accurately. It will be noticed that the results of the thick and the thin turbulent boundary-layer calculation methods differ appreciably (particularly with regard to the boundary-layer thickness and the shape-parameter) only in a small region near the tail of the bodies; but due to the lack of data in this region for the cases considered here, it is not possible to verify directly the conclusion of Patel (1973b), based on other more detailed experimental data, that the thick boundary-layer method represents a considerable improvement over the thin boundary-layer method of Shanebrook and Sumner. The use of the potential-flow pressure distribution also implies that the present calculations will not be as satisfactory in detail as those made by Patel using the experimental pressure distributions. The importance of using the thick boundary-layer method has, however, been remarked upon earlier in connection with the prediction of the drag coefficient using the Squire-Young method.

The drag coefficients (based on $S = V^{2/3}$, where V is the volume of the body), for the four bodies of revolution, calculated using the different transition criteria and the thin and thick boundary layer calculation methods are compared with the experimental values in Table 1. It will be seen that the most consistent results are obtained when (a) the location of the transition point coincides with the position observed experimentally and (b) the thick turbulent boundary-layer method of Patel (1973b) is employed. The reason for the over-estimation of the drag coefficient by the thin boundary-layer method in the case of Freeman and, to a lesser degree, in the case of the U.S. Navy Airship has already been discussed. The latter case also demonstrates that the precise location of transition becomes relatively unimportant at large Reynolds numbers since then the laminar boundary-layer flow is confined to a very small region close to the nose of the body.

Gertler (1950) has reported the results of deep-submergence resistance tests on a large number of bodies of revolution, known as the series 58 bodies, which were generated by systematically varying the fineness ratio, the prismatic coefficient, and the nose and tail radii (Landweber and Gertler (1950)). These tests were performed over a range of Reynolds numbers but the position of transition was fixed in all cases at X/L = 0.05 by means of sand-paper strips. The present procedure, i.e. using the thick turbulent boundary-layer method, was applied to calculate the drag coefficient of a representative number of these bodies. The results of the calculations are compared with the experimental data in Table 2 and shown in Figures 8(a) through 8(f). Note that here the drag coefficient is based on the total surface area. It will be seen that the present method again predicts the drag coefficient with acceptable accuracy.

IV. CONCLUDING REMARKS

The drag calculation method proposed and verified here is a more or less conventional one except for the treatment of the flow in the tail region of the body of revolution. Although the thick boundary layer over the tail portion is calculated by using an improved method, the drag calculation procedure remains an approximate one for two reasons: (1) the

potential-flow pressure distribution is used although this is not obtained in reality due to the interaction between the thick boundary layer and the external flow, and (2) the application of the drag formula of Granville in the manner suggested here means that the flow downstream of the point where the successive values of the drag coefficient reach a maximum does not have any influence on the final drag coefficient. The fact that the present method gives consistently accurate prediction of the drag for a wide variety of bodies of revolution does not, however, imply that the flow in the tail region of the body is unimportant. On the contrary, it indicates that the drag formulae suggested by Squire and Young, and Granville, which contain information concerning the pressure distribution and the boundary-layer parameters in the tail region, are in such a form that by regarding the flow in the tail region as a part of the wake they lead to a mutual cancellation of errors. The very fact that these formulae have stood the test of time vindicates this conclusion.

A more satisfactory procedure for the calculation of the drag of bodies of revolution can be developed by taking the flow in the tail region into account in a more direct and realistic manner. As pointed out by Patel (1973a), this will involve the following steps: (1) calculation of the thick boundary layer right up to the tail using the potential-flow pressure distribution on the body as a first approximation; (2) continuation of a boundary-layer type calculation through the near wake into the far wake; (3) calculation of the pressure, or velocity, distribution at the edge of the boundary layer and the wake by the application of potential-flow theory to the resulting semi-infinite domain; (4) evaluation of the pressure field between the body and the edge of the boundary layer and the wake from momentum considerations in the direction normal to the body surface; (5) a re-calculation of the boundary layer and the wake using this pressure field; and (6) iteration on the entire set of calculations until convergence is obtained. The drag on the body can then be found from the velocity and pressure variations across the boundary layer at the tail. The feasibility of such a procedure has not, however, been demonstrated conclusively so far. Apart from the convergence of such a scheme, major problems which may be encountered concern the development of methods which can calculate the near wake and the thick boundary layer across which there is a significant variation of static pressure. In the absence

of such a refined drag calculation procedure, however, methods based on Squire-Young type drag formulae, such as the present one, can be used with a fair degree of confidence.

REFERENCES

Cebeci, T., Mosinskis, G.J., and Smith, A.M.O., 1970, "Calculation of Viscous Drag and Turbulent Boundary-layer Separation on Two-Dimensional and Axisymmetric Bodies in Incompressible Flows", Douglus Aircraft Company, Report No. MDC J0973-01.

Cornish, J.J., and Boatwright, D.W., 1960, "Application of Full Scale Boundary Layer Measurements to Drag Reduction of Airships", Aerophysics Department, Mississippi State University, Report No. 28.

Crabtree, L.F., 1958, "Prediction of Transition in the Boundary Layer on Aerofoil", *J. Aeron. Sci., 52,* 525.

Freeman, H.B., 1932a, "Measurements of Flow in the Boundary Layer of a 1/40 - Scale Model of the U.S. Airship Akron", NACA Tech. Report No. 430.

Freeman, H.B., 1932b, "Force Measurements on a 1/40 - Scale Model of the U.S. Airship Akron", NACA Tech. Report No. 432.

Gertler, M., 1950, "Resistance Experiments on a Systematic Series of Streamlined Bodies of Revolution -- For Application to the Design of High-Speed Submarines", David Taylor Model Basin, Report No. 849.

Granville, P.S., 1953, "The Calculation of Viscous Drag of Bodies of Revolution", David Taylor Model Basin, Report No. 849.

Hall, D.J., and Gibbings, J.C., 1972, "Influence of Stream Turbulence and Pressure Gradient upon Boundary Layer Transition", *J. Mech. Eng. Sci., 14,* 134.

Head, M.R., 1958, "Entrainment in the Turbulent Boundary Layer", British Aeron. Res. Counc., R & M 3152.

Jaffe, N.A., Okamura, T.T., and Smith, A.M.O., 1970, "Determination of Spatial Amplification Factors and their Application to Predicting Transition", *AIAA Journal 8,* 301.

Landweber, L., 1959, "Potential Flow About Bodies of Revolution and Symmetric Two-Dimensional Flows", Iowa Institute of Hydraulic Research, BuShips Index No. NS 715-102.

Landweber, L., and Gertler, M., 1950, "Mathematical Formulation of Bodies of Revolution", David Taylor Model Basin Report No. 719.

Lyon, H.m., 1934, "Flow in the Boundary Layer of Streamline Bodies", British Aeron. Res. Counc., R & M, 1622.

Michel, R., 1951, "Etude de la Transition sur les Profiles d'aile; Establissement d'un Critere de Determination du Point de Transition et Calcul de la Trainee de Profile Incompressible", O.N.E.R.A. Report 1/1578A.

Nash, J.F., 1965, "Turbulent Boundary-Layer Behavior and the Auxiliary Equation", British Aeron. Res. Counc., C.P. 835.

Patel, V.C., 1973a, "On the Equations of a Thick Axisymmetric Turbulent Boundary Layer", Iowa Institute of Hydraulic Research, Report No. 143.

Patel, V.C., 1973b, "A Simple Integral Method for the Calculation of Thick Axisymmetric Turbulent Boundary Layers", Iowa Institute of Hydraulic Research, Report No. 150.

Patel, V.C., Nakayama, A. and Damian, R., 1973, "An Experimental Study of the Thick Turbulent Boundary Layer Near the Tail of a Body of Revolution", Iowa Institute of Hydraulic Research, Report No. 142. (Also, to be published in the *J. Fluid Mechanics*.)

Parsons, J.S., and Goodson, R.E., 1972, "The Optimum Shaping of Axisymmetric Bodies for Minimum Drag in Incompressible Flow", Automatic Control Center, School of Mech. Eng., Purdue University, Report No. ACC-72-5.

Rott, N., and Crabtree, L.F., 1952, "Simplified Laminar Boundary-Layer Calculations for Bodies of Revolution and for Yawed Wings", *J. Aeron. Sci., 19,* 553.

Shanebrook, J.R., and Sumner, W., 1970, "Entrainment Theory for Axisymmetric Turbulent Incompressible Boundary Layers", *AIAA, J. Hydronautics, 4,* 159.

Thompson, B.G.J., 1965, "A New Two-Parameter Family of Mean Velocity Profiles for Incompressible Turbulent Boundary Layers on Smooth Walls", British Aeron. Res. Counc., R & M 3463.

Thwaites, B., 1949, "Approximate Calculation of the Laminar Boundary Layer", *Aero. Quart., 1,* 245.

Van Ingen, J.L., 1956, "A Suggested Semi-Empirical Method for the Calculation of the Boundary Layer Transition Region", Report No. V.T.H. 74, Delft, Holland

Van Driest, E.R., and Blumer, C.B., 1963, "Boundary Layer Transition: Freestream Turbulence and Pressure Gradient Effects", *AIAA Journal 1,* 1303.

Young, A.D., 1939, "The Calculation of the Total and Skin Friction Drags of Bodies of Revolution at Zero Incidence", British Aeron. Res. Counc., R & M 1874.

	$R_e = \frac{U_\infty L}{\nu}$	Experiment		Method of Transition Prediction: Experimental X_{tr}		Michel's Method		Granville's Method		Van Driest and Blumer's Method		Crabtree's Method	
		X_{tr}/L	C_D	X_{tr}/L	C_D	X_{tr}/L	C_D	X_{tr}/L	C_D	X_{tr}/L	C_D	X_{tr}/L	C_D
Freeman's Akron Model	1.73×10^7	$0.06 \sim 0.07$	0.0190 (wooden) 0.0219 (metal)	0.070	0.0198	0.552	0.0100	0.272	0.0161	0.252	0.0165	0.262	0.0163
Lyon's Model A	2.04×10^6	$0.5 \sim 0.7$	0.0142	0.60	0.0132 (0.0134)	0.592	0.0135 (0.0137)	0.632	0.0123 (0.0125)	0.632	0.0123 (0.0125)	0.612	0.0129 (0.0131)
Lyon's Model B	2.04×10^6	$0.25 \sim 0.35$	0.0236	0.332	0.0218 (0.0223)	0.652	0.0132 (0.0135)	0.722	0.0113 (0.0115)	0.732	0.0110 (0.0113)	0.722	0.0113 (0.0115)
U.S. Navy ZS2G-1 Airship	1.77×10^8	Not Known	0.0125	—	—	Not Applicable		0.160	0.0113 (0.0129)	0.06	0.0122 (0.0140)	0.132	0.0116 (0.0133)

( ) calculated using thin boundary layer method

Table 1. Experimental and Calculated Drag Coefficients Using Various Transition Criteria

Model	Position of r_{max} m $= \frac{X_m}{L}$	Nose Radius R_n $= \frac{r_n L}{d^2}$	Tail Radius R_t $= \frac{r_t L}{d^2}$	Prismatic Coefficient C_P $= \frac{4V}{\pi d^2 L}$	Fineness Ratio L/d	Reynolds Number R_e x 10^{-6}	Experimental $C_D x 10^3$	Calculated $C_D x 10^3$
4154	0.40	0.50	0.10	0.65	4.0	20.0	3.21	3.114
4155	0.40	0.50	0.10	0.65	5.0	20.0	2.99	2.948
4156	0.40	0.50	0.10	0.65	6.0	20.0	2.85	2.846
4157	0.40	0.50	0.10	0.65	7.0	2.85	3.87	3.905
4157	0.40	0.50	0.10	0.65	7.0	5.70	3.39	3.445
4157	0.40	0.50	0.10	0.65	7.0	7.10	3.27	3.318
4157	0.40	0.50	0.10	0.65	7.0	11.00	3.16	3.088
4157	0.40	0.50	0.10	0.65	7.0	14.20	2.99	2.966
4157	0.40	0.50	0.10	0.65	7.0	17.10	2.87	2.883
4157	0.40	0.50	0.10	0.65	7.0	19.80	2.79	2.818
4157	0.40	0.50	0.10	0.65	7.0	20.00	2.76	2.780
4157	0.40	0.50	0.10	0.65	7.0	22.70	2.66	2.763
4158	0.40	0.50	0.10	0.65	8.0	20.0	2.72	2.733
4159	0.40	0.50	0.10	0.65	10.0	20.0	2.70	2.674
4160	0.36	0.50	0.10	0.65	7.0	20.0	2.75	2.779
4161	0.44	0.50	0.10	0.65	7.0	20.0	2.78	2.781
4162	0.48	0.50	0.10	0.65	7.0	20.0	2.80	2.784
4163	0.52	0.50	0.10	0.65	7.0	20.0	2.82	2.788
4164	0.40	0.50	0.10	0.55	7.0	20.0	3.00	2.785
4165	0.40	0.50	0.10	0.60	7.0	20.0	2.70	2.775
4166	0.40	0.50	0.10	0.70	7.0	20.0	2.91	2.801
4167	0.40	0.00	0.10	0.65	7.0	20.0	2.79	2.819
4168	0.40	0.30	0.10	0.65	7.0	20.0	2.77	2.791
4169	0.40	0.70	0.10	0.65	7.0	20.0	2.77	2.773
4170	0.40	1.00	0.10	0.65	7.0	20.0	2.81	2.769
4171	0.40	0.50	0.00	0.65	7.0	20.0	2.76	2.789
4172	0.40	0.50	0.05	0.65	7.0	20.0	2.76	2.783
4173	0.40	0.50	0.15	0.65	7.0	20.0	2.76	2.778
4174	0.40	0.50	0.20	0.65	7.0	20.0	2.73	2.776
4175	0.40	0.50	0.10	0.60	5.0	20.0	2.95	2.933
4176	0.40	0.50	0.10	0.55	5.0	20.0	3.04	2.956
4177	0.34	0.50	0.10	0.65	7.0	20.0	2.79	2.780

Table 2. Experimental and Calculated Drag Coefficients (based on the Wetted Surface Area) for the Series 58 Bodies of Revolution

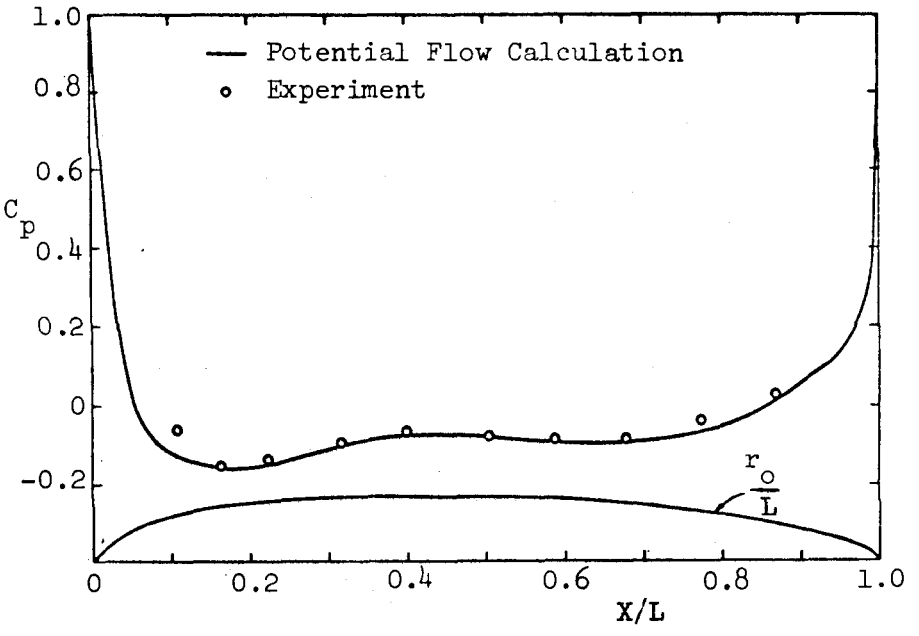

(a) Model of Airship Akron, Freeman (1932)

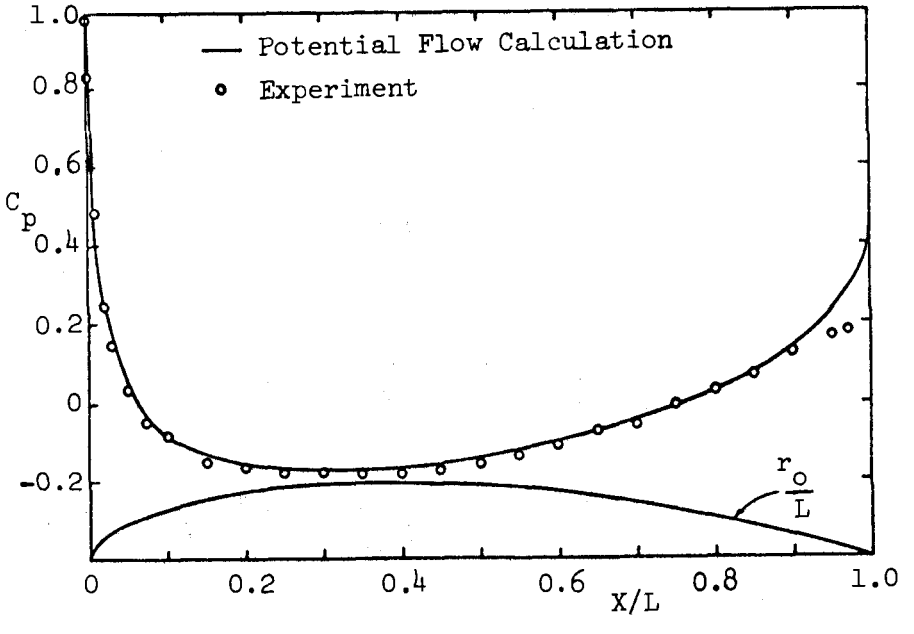

(b) Model B of Lyon (1934)

Figure 1. Comparison Between Experimental and Potential Flow Pressure Distributions

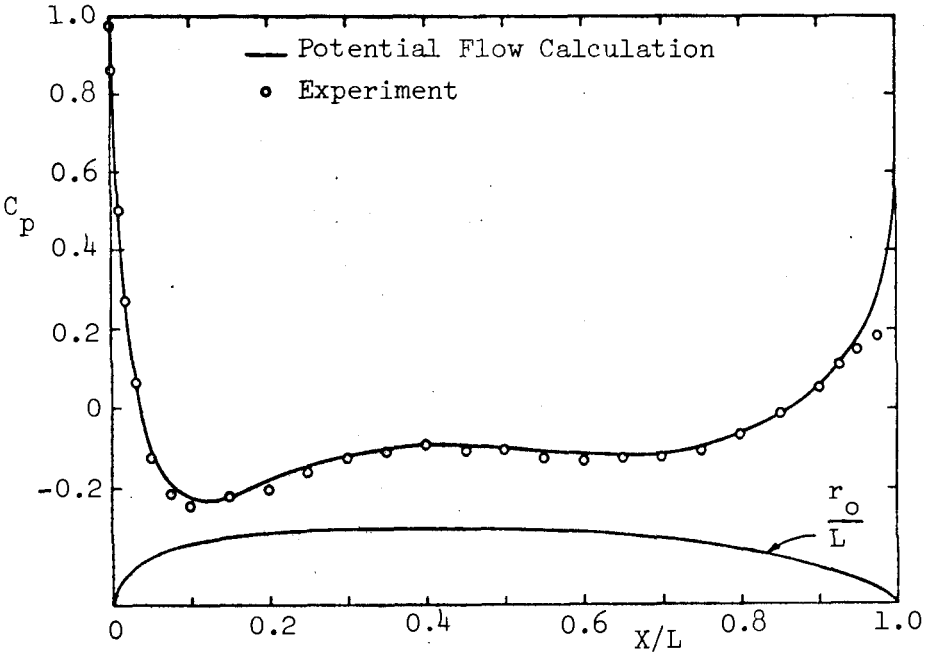

(c) Model A of Lyon (1934)

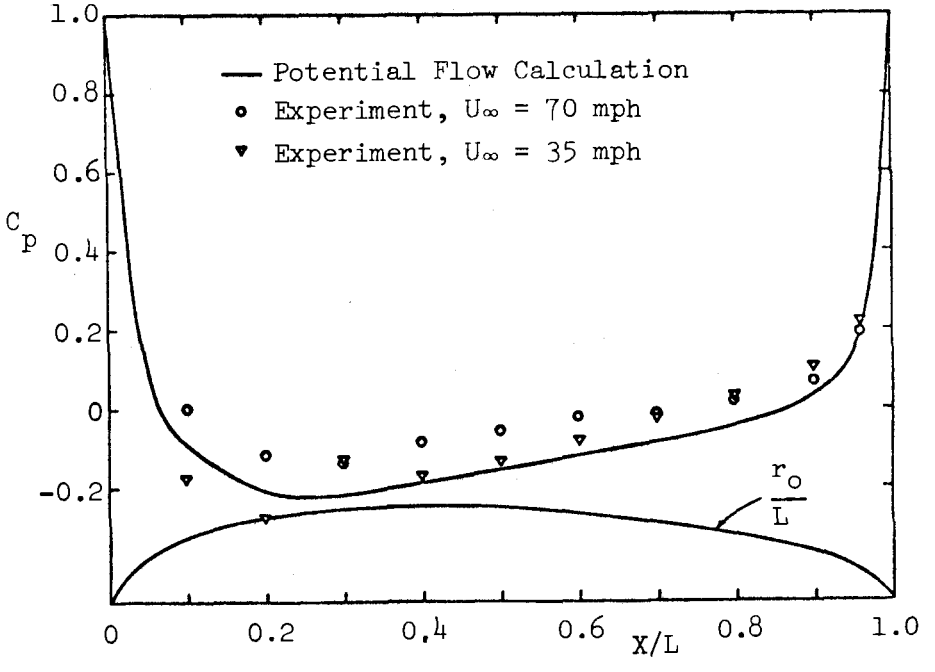

(d) U.S. Navy Airship, Cornish and Boatwright (1960)

Figure 1. (Continued)

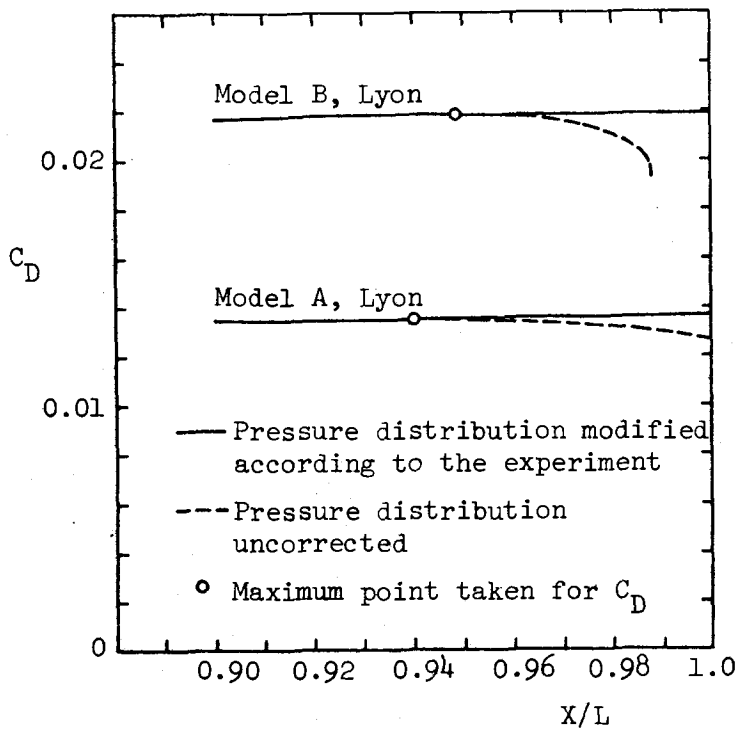

Figure 2. Determination of Drag Coefficient by the Use of Granville's Formula After Each Step in the Boundary Layer Calculation

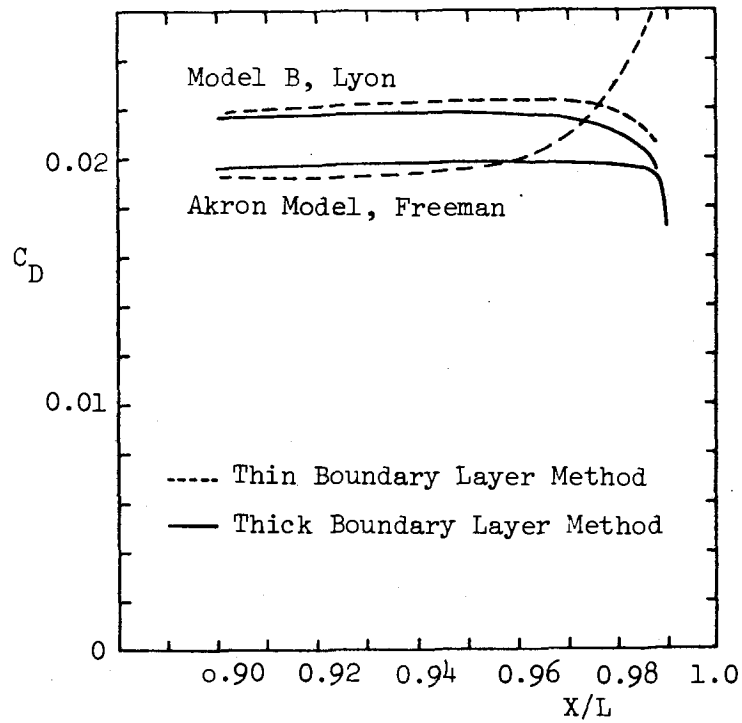

Figure 3. Variation of Drag Coefficient Using the Thin and Thick Boundary Layer Calculation Method

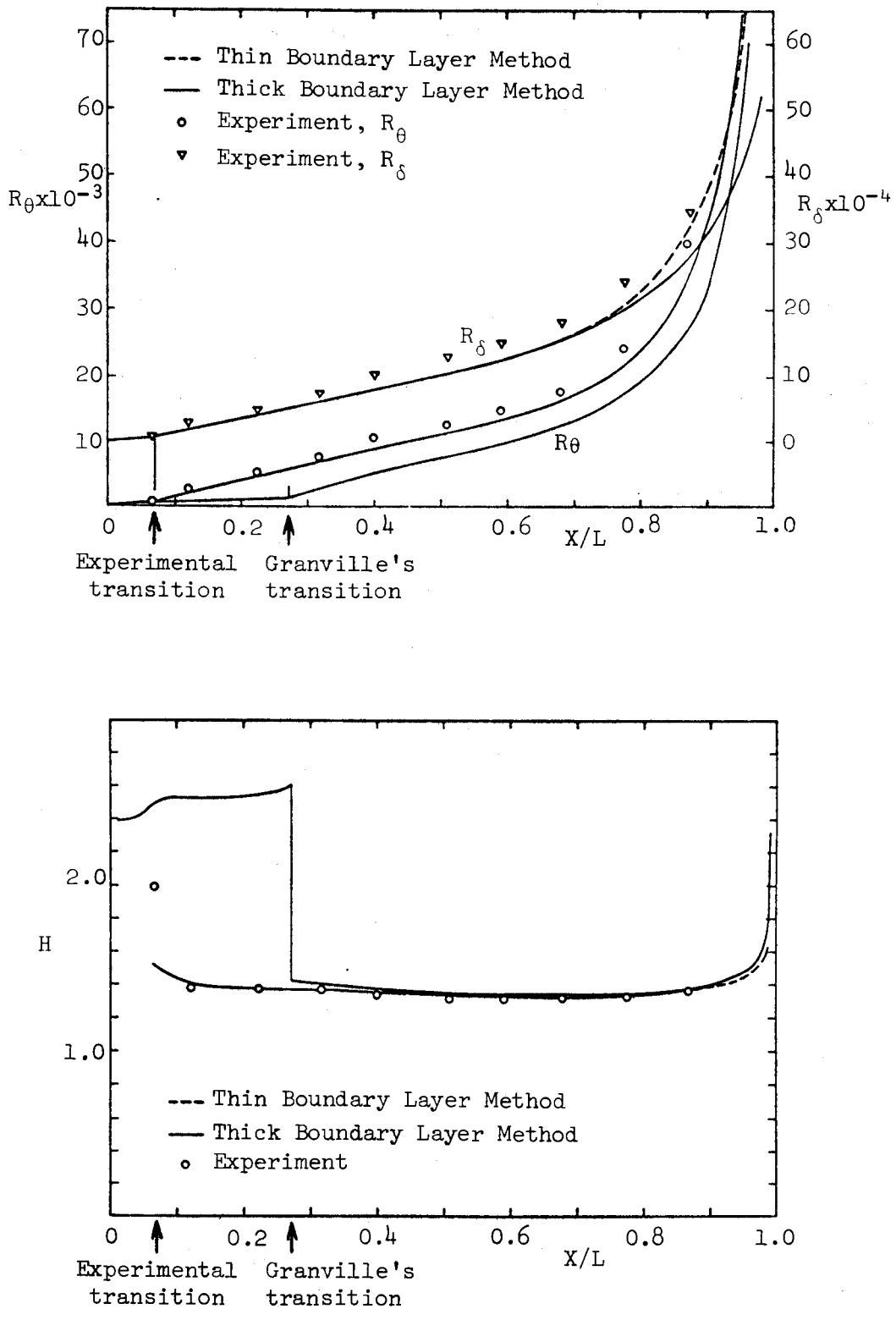

Figure 4. Experimental and Calculated Boundary Layer Development: Airship Akron, Freeman (1932)

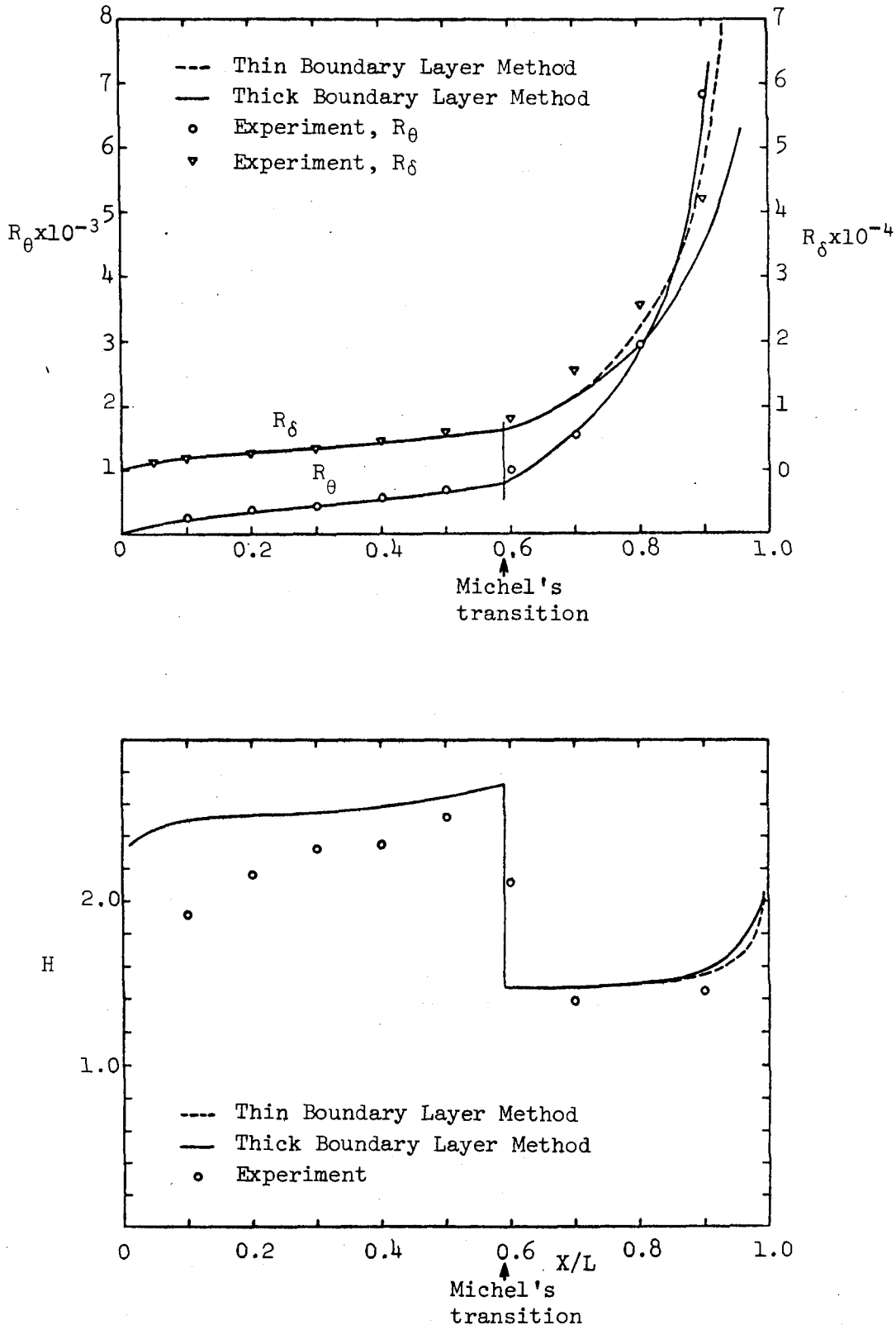

Figure 5. Experimental and Calculated Boundary Layer Development: Model A, Lyon (1934)

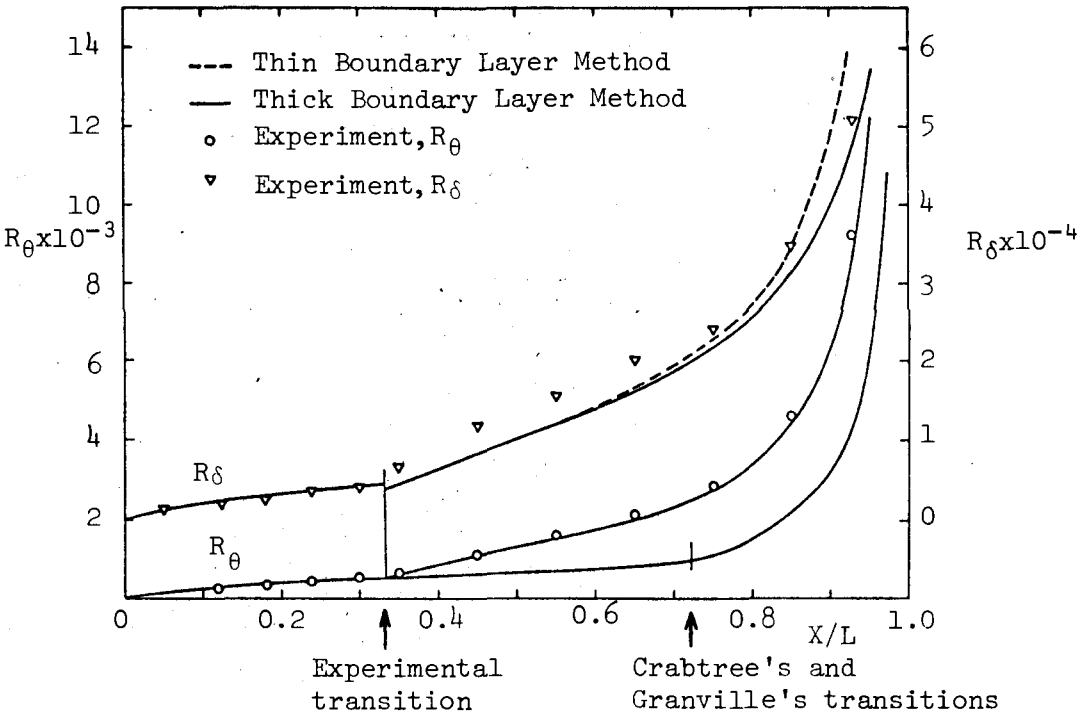

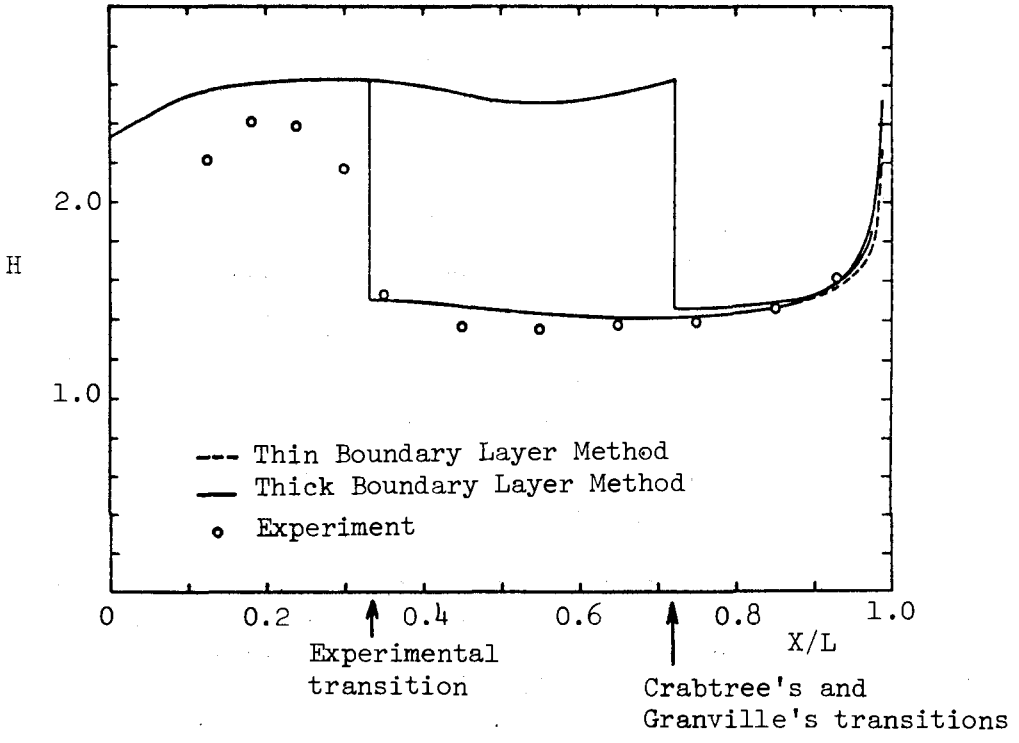

Figure 6. Experimental and Calculated Boundary Layer Development: Model B, Lyon (1934)

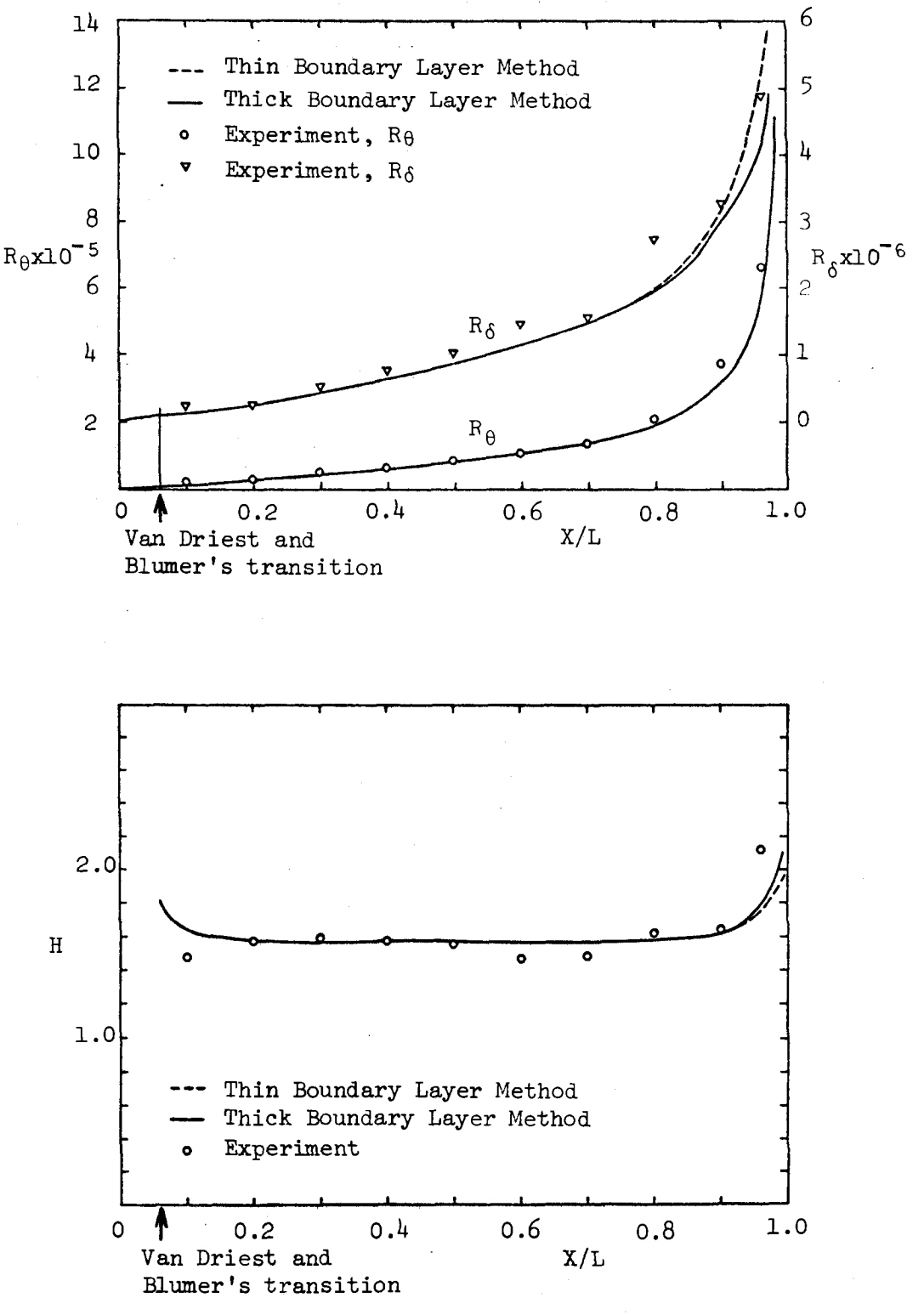

Figure 7. Experimental and Calculated Boundary Layer Development: U.S. Navy Airship, Cornish and Boatwright (1960)

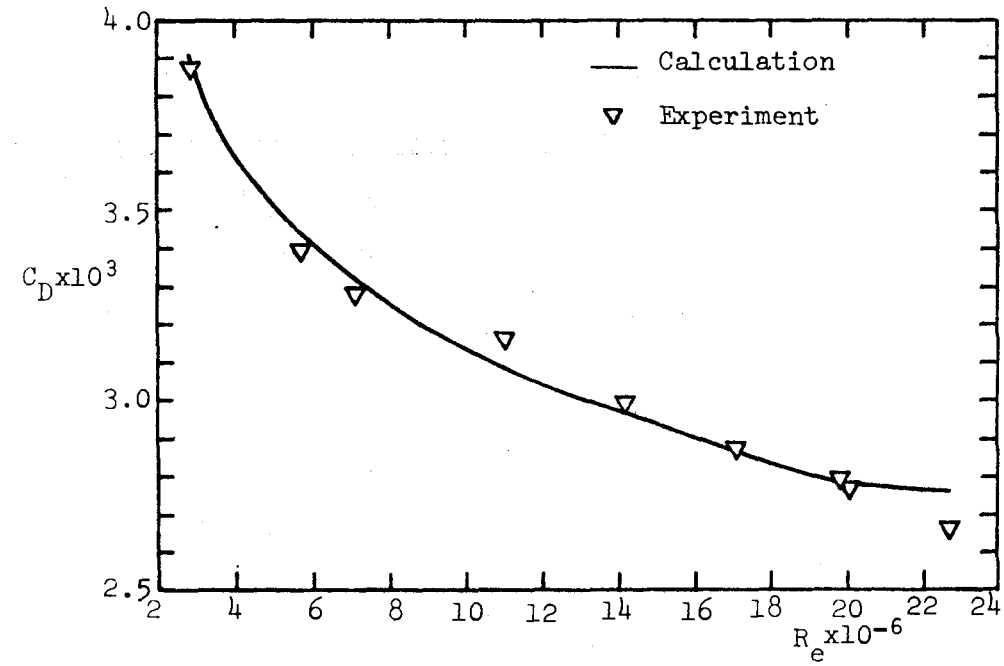

(a) Influence of Reynolds number

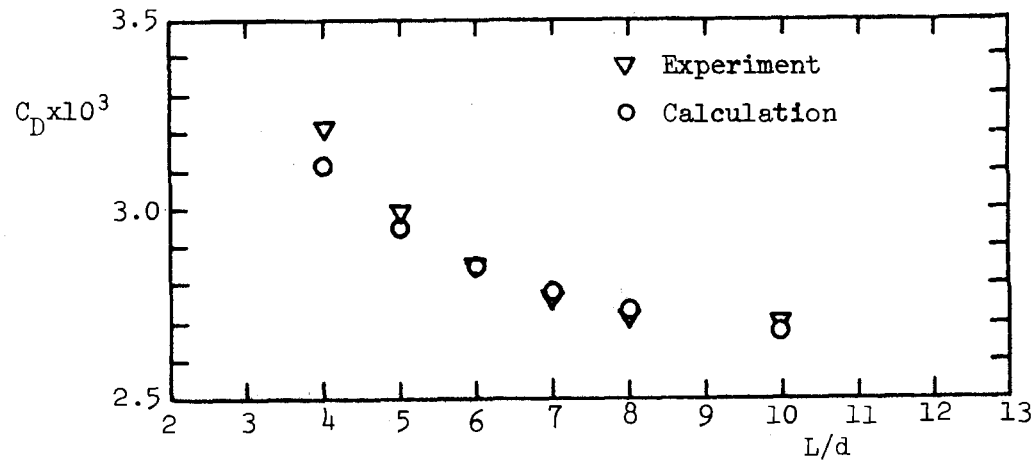

(b) Influence of Fineness Ratio

Figure 8. Drag Coefficients ($C_D = \frac{D}{\frac{1}{2}\rho U_\infty^2 S}$) of the Series 58 Bodies of Gertler (1950)

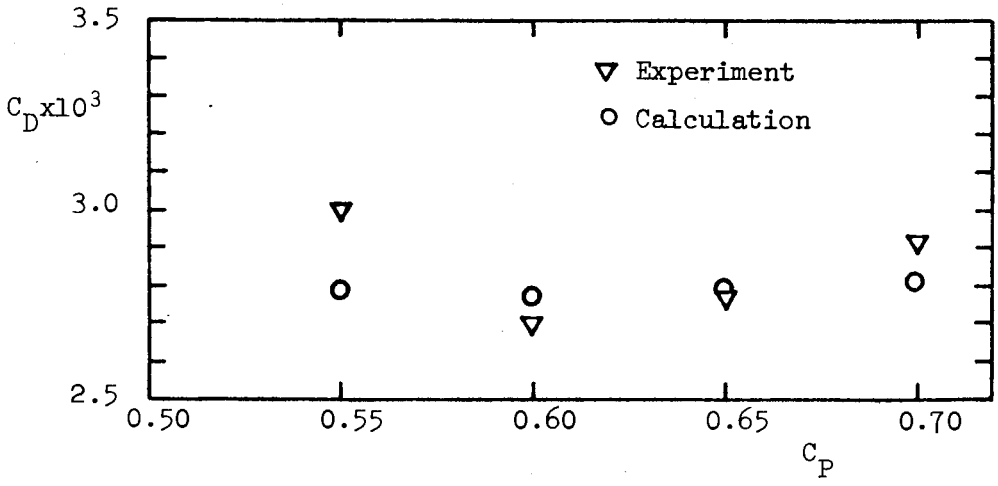

(c) Influence of Prismatic Coefficient

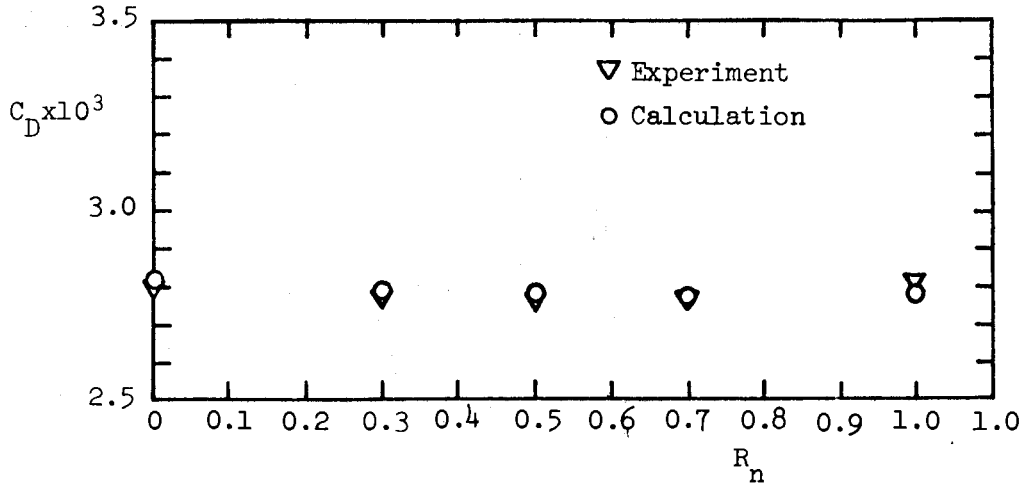

(d) Influence of Nose Radius

Figure 8. (Continued)

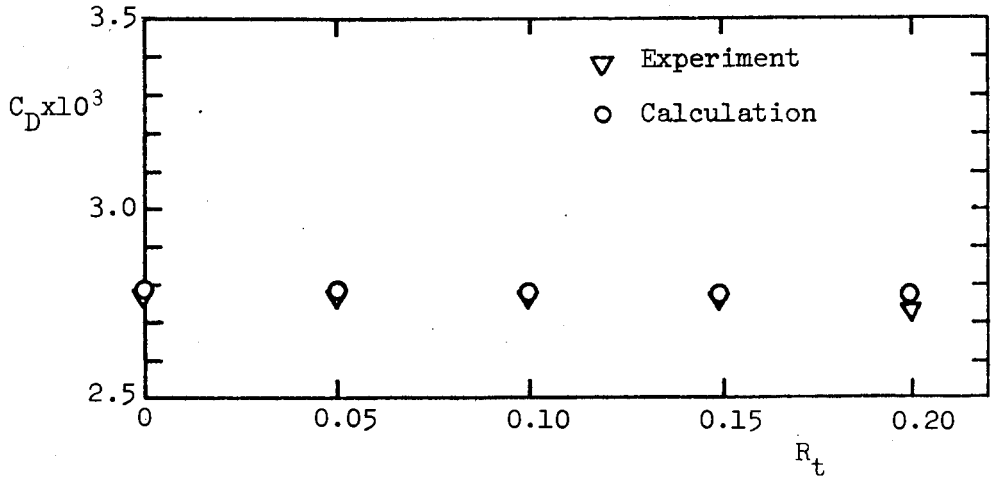

(e) Influence of Tail Radius

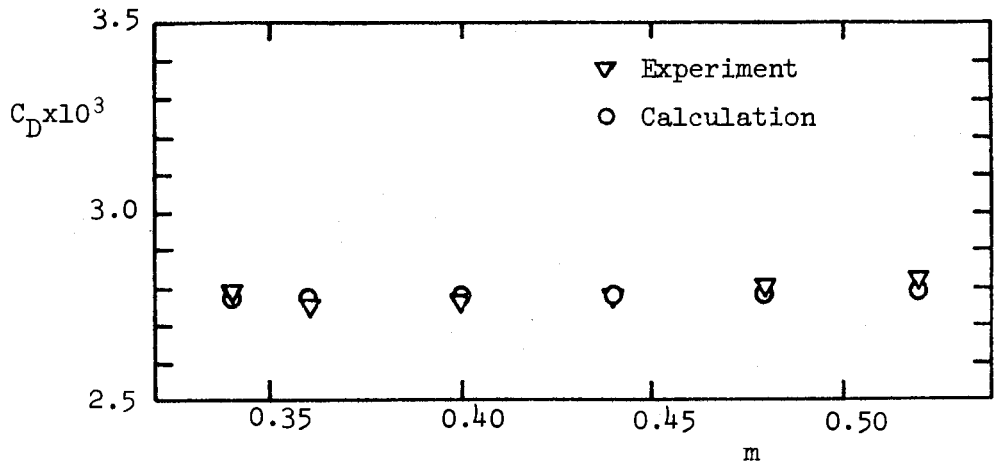

(f) Influence of Position of Maximum Radius

Figure 8. (Continued)

NSRDC LIST

December 5, 1973

Docs/Repts/Trans Section
Scripps Inst. of Oceanography Library
University of Calif., San Diego
P.O. Box 2367
La Jolla, Calif. 92037

University of Calif. at San Diego
La Jolla, Calif. 92038
Attn: Dr. A.T. Ellis
Dept. of Applied Math

2 McDonnell Douglas Aircraft Co.
Attn: A.M.O. Smith, J. Hess
3855 Lakewood Blvd.
Long Beach, Calif. 90801

Stanford Research Institute
Menlo Park
California 94502

3 Naval Postgraduate School
Monterey, Calif. 93940
Attn: Library, Code 2124
Attn: Dr. T. Sarpkaya
Attn: Prof. J. Miller

Nielsen Engineering & Research, Inc.
850 Maude Avenue
Attn: Mr. S.B. Spangler
Mountain View, Calif. 94040

2 Officer-In-Charge
Naval Undersea Research and
Development Center
Attn: Dr. J. Hoty (2501) Library
Pasadena, Calif. 91107

Commanding Officer (131)
Naval Civil Engineering Lab
Port Hueneme, Calif. 93043

Commander
Naval Undersea Research and
Development Center
Attn: Dr. A. Fabula (6005)
San Diego, Calif. 92132

Commander
Electronics Laboratory Center
(Library)
San Diego, Calif. 92125

Director
Office of Naval Research
Branch Office
50 Fell Street
San Franciso, California 94102

Hunters Point Naval Shipyard
Technical Library (Code 202.3)
San Francisco, Calif. 94135

2 Stanford University
Attn: Engineering Library
Dr. R. Street
Stanford, Calif. 94305

Lockheed Missiles & Space Co.
P.O. Box 504
Attn. Mr. R.L. Waid, Dept. 57-74
Bldg. 150, Facility 1
Sunnyvale, Calif. 94088

Mare Island Naval Shipyard
Shipyard Technical Library
Code 202.3
Vallejo, Calif. 94592

Assistant Chief Design Engineer
For Naval Architecture (Code 250)
Mare Island Naval Shipyard
Vallejo, California 94592

Colorado State University
Foothills Campus
Fort Collins, Colorado 80521
Attn: Reading Room
Engr. Res. Center

University of Bridgeport
Attn. Prof. Earl Uram
Mechanical Engineering Dept.
Bridgeport, Conn. 06602

Electric Boat Division
Attn: Mr. V. Boatwright, Jr.
General Dynamics Corporation
Groton, Connecticut 03640

University of Connecticut
Box U-37
Storrs, Conn. 06268
Attn: Dr. V. Scottron
Hydraulics Res. Lab

2 Florida Atlantic University
Ocean Engineering Dept.
Attn: Technical Library
Dr. S. Dunne
Boca Raton, Florida 33432

Director
Naval Research Lab
Underwater Sound Ref. Division
P.O. Box 8337
Orlando, Florida 32806

University of Hawaii
Dept. of Ocean Engineering
2565 The Mall
Attn: Dr. C. Bretschneider
Honolulu, Hawaii 96822

University of Illinois
Urbana, Illinois 61801
Attn: Dr. J. Robertson

2 College of Engineering
University of Notre Dame
Notre Dame, Indiana 46556
Attn: Engineering Library
Attn: Dr. A. Strandhagen

University of Kansas
Chm., Civil Engr. Dept. Library
Lawrence, Kansas 66044

Kansas State University
Engineering Experiment Station
Seaton Hall
Manhattan, Kansas 66502
Attn: Prof. D. Nesmith

Officer-in charge
Naval Ship Research and Development
Laboratory
Annapolis, Maryland 21402
Attn: Library

3 U.S. Naval Academy
Annapolis, Md. 21402
Attn: Technical Library
Attn: Dr. Bruce Johnston
Attn: Profe. P. Van Mater, Jr.

The John Hopkins University
Baltimore, Md. 21218
Attn: Prof. O. Phillips
Mech. Depts.

40 Commander
Naval Ship Res. and Devel. Center
Attn: Code 1505
Code 5614 (39 cys)
Bethesda, Maryland 20034

8 Commander
Naval Ship Engineering Center
Dept. of the Navy Center Bldg.
Prince Georges Center
Hyattsville, Maryland 20782
Sec 6034B, 6110, 6114H, 6120, 6136
6144G, 6140B, 6148

2 Hydronautics, Incorporated
Attn: Library
Attn: Mr. Gertler
Pindell School Road
Howard County
Laurel, Maryland 20810

Bethlehem Steel Corporation
Attn: Mr. A. Haff, Technical Mgr.
Central Technical Division
Sparrows Point Yard
Sparrows Point, Maryland 21219

Bolt, Beranek and Newman
Attn: Library
50 Moulton Street
Cambridge, Mass. 02138

Bolt, Beranek and Newman
1501 Wilson Bovd
Arlington, Virginia 22209
Attn: Dr. F. Jackson

Cambridge Acoustical Associates, Inc.
1033 Mass. Avenue
Cambridge, Mass. 02138
Attn: Dr. M. Junger

2 Harvard University
Pierce Hall
Cambridge, Mass. 02138
Prof. G. Carrier
Gordon McKay Library

5 Massachusetts Inst. of Technology
Dept. Ocean Engineering
Attn: Library, Prof. P. Mandel, Dr. Leehey
Attn: Prof. M. Abkowitz, Dr. J. Newman
Cambridge, Massachusetts 02159

Parsons Lab, Prof. A. Ippen
M.I.T.
Cambridge, Mass. 02319

Attn: Reference Room
Woods Hole Oceanographic Inst.
Woods Hole, Mass. 02543

Worcester Polytechnic Inst.
Alden Research Lab
Attn: Technical Library
Worcester, Mass. 06109

3 University of Michigan
Attn: Dr. T.F. Ogilvie, Prof. F. Hammit
Dept. of Naval Architecture
and Marine Engineering
Ann Arbor, Michigan 48105

5 St. Anthony Falls Hydraulic Lab.
University of Minnesota
Mississippi River at 3rd Ave., S.E.
Minneapolis, Minn. 55414
Attn: Director
Attn: Mr. J. Wetzel, Mr. F. Schiebe
Attn: Mr. J. Killen, Dr. C. Song

Research Center Library
Waterways Experiment Station
Corps of Engineers
P.O. Box 631
Vicksburg, Mississippi 39180

3 Davidson Lab
Stevens Institute of Technology
711 Hudson Street
Hoboken, New Jersey 07030
Mr. J. Breslin, Mr. S. Tsakonas
Attn: Library

Depart. of Aerospace and
Mechanical Sciences
Princeton University
Princeton, New Jersey 08540
Attn: Prof. G. Mellor

New York University, W. Pierson, Jr.
University Heights
Bronx, New York 10453

Cornell Aeronautical Lab
Aerodynamics Research Dept.
P.O. Box 235
Buffalo, New York 14221
Attn: Dr. A. Ritter

Long Island University
Graduate Dept. of Marine Science
40 Merrick Avenue
East Meadow, New York 11554
Attn: Prof. David Price

3 Webb Inst. of Naval Arch.
Attn. Prof. E.V. Lewis, Library
Prof. L.W. Ward
Crescent Beach Road
Glen Cove, L.I., New York 11542

Cornell University
Graduate School of Aerospace Engr.
Ithaca, New York 14850
Attn: Prof. W.R. Sears

U.S. Merchant Marine Academy
Attn: Academy Library
Kings Points, L.I., New York 11204

U.S. Merchant Marine Academy
Attn. Cap. L.S. McCready, Head
Department of Engineering
Kings Point, L.I., N.Y. 11024

Dept. of Mathematics
St. Johns University
Jamaica, New York 11432
Attn: Prof. J. Lurye

Sperry Systems Management Div.
Sperry Gyroscope Co.
Great Neck
Long Island, New York 11020

Bethlehem Steel Company
25 Broadway
New York, New York 10004
Attn. Library (Shipbuilding)

Eastern Research Group
P.O. Box 222
Church Street Station
New York, New York 10008

ESSO International
Attn. Mr. R. J. Taylor
Const. and Develop. Div.
Tanker Department
15 West 51 Street
New York, New York 10019

2 New York University
Courant Inst. of Math. Sciences
251 Mercier St.
New York, New York 10012

Technical Inf. Control Section
Gibbs and Cox, Inc.
21 West Street
New York, New York 10006

FFOL/FYS (J. Olsen)
Wright Patterson AFB
Dayton, Ohio 45433

Fritz Engr. Lab Library
Dept. of Civil Engr.
Legigh University
Bethlehem, Pa. 18015

Sun Shipbuilding and DD Company
Attn. Chief Naval Architect
Chester, Pa. 19013

Commander
Philadelphia Naval Shipyard
Attn: Code 240
Philadelphia, Pennsylvania 19112

Library
The Pa. State University
Ordnance Research Lab
P.O. Box 30
State College, Pennsylvania 16801

2 Director
Attn: Dr. G. Wislicenus
Ordnance Research Lab.
Pennsylvania State University
University Park, Pennsylvania

Commanding Officer
U.S. Naval Air Development
Center Johnsville
Warminster, Pennsylvania 18974

Library
Naval Underwater Systems Center
Newport, Rhode Island 02840

Applied Research Lab Library
University of Texas
P.O. Box 8029
Austin, Texas 78712

Tracor Incorporated
6500 Tracor Lane
Austin, Texas 78721

2 Southwest Research Institute
8500 Colegra Road
Applied Mechanics REview
Attn: Dr. H. Abramson
San Antonio, Texas 78206

College of Engineering
Utah State University
Logan, Utah 84321
Attn: Dr. R. Jeppson

12 Director
Defense Documentation Center
5010 Duke Street
Alexandria, Virginia 22314

Office of Naval Research
800 N. Quincy Street
Arlington, Virginia 22217
Attn: Mr. R.D. Cooper (Code 438)

AFOSR/NAM
1400 Wilson Blvd.
Arlington, Virginia 22209

Technical Library
Naval Proving Ground
Dehlgren,
Virginia 22448

Robert Taggart, Inc.
Attn. Mr. Robert Taggart
3930 Walnut Street
Fairfax, Virginia 22030

Newport News Shipbuilding
Attn: Technical Library Dept.
4101 Washington Avenue
Newport News, Virginia 23607

Naval Ship Engineering Center
Norfolk Division
Small Craft Engr. Dept.
Attn: D. Blount (6660.03)
Norfolk, Virginia 23511

Engineering Library
Puget Sound Naval Shipyard
Bremerton, Washington 98314

Applied Physics Lab
University of Washington
1013 N.E. 40th Street
Attn: Technical Library
Seattle, Washington 98105

Catholic University of America
Attn: Dr. S. Heller
Dept. of Civil & Mech. Engr.
Washington, D.C. 20017

Commander
Naval Facilities Engineering Command
Code 032C
Washington, D.C. 20390

Commander
Naval Oceanographic Office
Library
Department of the Navy
Washington, D.C. 20390

Commander
Naval Ordance Systems
Command (ORD 035)
Washington, D.C. 20360

5 Commander
Naval Ship Systems Command
Washington, D.C. 20360
Ships 2052 (3 Cys), Ships 03412B
Ships 0372,

Dept. of Transportation
Library TAD-491.1
400 7th Street, S.W.
Washington,D.C. 20590

Dept. of Transportation Library
Acquisitions Section, TAD 491.1
400 7th Street, S.W.
Washington, D.C. 20590

2 Director
Attn: Library
Attn: Code 2027, 2629 (ONRL)
U.S. Naval Research Lab.
Washington, D.C. 20390

2 National Bureau of Standards
Washington, D.C. 20234
Attn: P. Klebanoff (FM 105)
Fluid Mechanics
Hydraulics Section

National Science Foundation
Engineering Division Library
1800 G. Street, N.W.
Washington, D.C. 20550

3 California Inst. of Tech.
Attn: Aeronautics Library
Attn: Dr. T.Y. Wu
Attn: Dr. A.J. Acosta
Pasadena, Calif. 91109

Chief Scientist
Office of Naval Research
Branch Office
1030 East Green Street
Pasadena, Calif. 91101

Technical Library
Charleston Naval Shipyard
U.S. Naval Base
Charleston, South Carolina 29408

Technical Library
Norfolk Naval Shipyard
Portsmouth, Virginia 23709

Commander
Pearl Harbor Naval Shipyard
Box 400
Attn: Code 202.32
FPO San Francisco, Calif. 96610

Technical Library
Portsmouth Naval Shipyard
Portsmouth, New Hampshire 03804

Commanding Officer
Office of Naval Research
Branch Office
495 Summer Street
Boston, Mass. 02210

Commanding Officer
Office of Naval Research
Branch Office Chicago
536 South Clark Street
Chicago, Illinois 60605

Library of Congress
Science and Technology Div.
Washington, D.C. 20540

Oceanics, Incorporated
Dr. Paul Kaplan
Technical Inudstrial Park
Plainview,L.I., New York 11803

Office of Naval Research
Area Office - Scientific Section
207 West 24 Street
New York, New York 10011

Planning Dept. Bldg. 39
Technical Library, Code 202.2
Boston Naval Shipyard
Boston, Mass. 02129

Society of Naval Architects
and Marine Engineers
74 Trinity Place
New York, New York 10004

Technical Library (246L)
Long Beach Naval Shipyard
Long Beach, Calif. 90801

4 University of California
Naval Architecture Department
Attn: Prof. J.V. Wehausen
Attn: Library
Attn: J. Paulling, W. Webster
Berkeley, Calif. 94720

North American Aviation, Inc.
Space & Information Systems Div.
Attn: Mr. Ben Ujihara (SL-20)
12214 Lakewood Blvd.
Downey, Calif. 90241

Unclassified

Security Classification

DOCUMENT CONTROL DATA - R & D

(Security classification of title, body of abstract and indexing annotation must be entered when the overall report is classified)

1. ORIGINATING ACTIVITY (Corporate author)

Institute of Hydraulic Research
The University of Iowa
Iowa City, Iowa 52242

2a. REPORT SECURITY CLASSIFICATION

Unclassified

2b. GROUP

3. REPORT TITLE

"Calculation of the Viscous Resistance of Bodies of Revolution"

4. DESCRIPTIVE NOTES (Type of report and, inclusive dates)

IIHR Report No. 151

5. AUTHOR(S) (First name, middle initial, last name)

A. Nakayama and V.C. Patel

6. REPORT DATE	7a. TOTAL NO. OF PAGES	7b. NO. OF REFS
October 1973	33	26

8a. CONTRACT OR GRANT NO.	9a. ORIGINATOR'S REPORT NUMBER(S)
N00014-68-A-0196-0002	IIHR Report No. 151
b. PROJECT NO.	
c.	9b. OTHER REPORT NO(S) (Any other numbers that may be assigned this report)
d.	

10. DISTRIBUTION STATEMENT

Approved for public release; distribution unlimited

11. SUPPLEMENTARY NOTES	12. SPONSORING MILITARY ACTIVITY
	Naval Ship Research & Development Center Bethesda, Maryland

13. ABSTRACT

The flow in the tail region of a body of revolution is a complex one since there the boundary layer often grows to a thickness many times the local radius of the body and there results a strong interaction between the boundary layer and the external potential flow. The influence of making simplifying assumptions concerning the flow in this region in conventional drag-calculation methods is discussed, and assessed by incorporating a method which takes into account the effects of the thick axisymmetric boundary-layer near the tail in an approximate manner. It is shown that this modification leads to a drag-calculation method which gives consistently accurate prediction of the viscous resistance of a wide variety of bodies of revolution.

DD FORM 1 NOV 65 1473 (PAGE 1)

S/N 0101-807-6811

Unclassified

Security Classification

A-31408

14. KEY WORDS	LINK A		LINK B		LINK C	
	ROLE	WT	ROLE	WT	ROLE	WT
Bodies of Revolution						
Viscous Resistance						
Boundary Layer Calculations						
Laminar Flow						
Turbulent Flow						
Transition Criteria						
Potential Flow Calculations						